3D Directional Temperature Responsive (*N*-(DL)-(1-Hydroxymethyl) Propylmethacrylamide-*co*-*n*-butyl Acrylate) Colloids and Their Coalescence

Fang Liu and Marek W. Urban*

Shelby F. Thames Polymer Science Research Center, School of Polymers and High Performance Materials, The University of Southern Mississippi, Hattiesburg, Mississippi 39406

Received September 18, 2007; Revised Manuscript Received November 7, 2007

ABSTRACT: A new family of colloidal dispersions containing *N*-(DL)-(1-hydroxymethyl) propylmethacrylamide (DL-HMPMA) and *n*-butyl acrylate (nBA) monomers was developed which exhibits temperature-responsive behavior. Particle size analysis, along with UV−vis and ^{1}H NMR spectroscopic measurements, showed that aqueous p(DL-HMPMA/nBA) particle dispersions display second-order lower critical solution temperature (II-LCST) in the 27−37 °C range at which the particle size decreases from 81 to 47 nm. When p(DL-HMPMA/nBA) colloidal particles were coalesced to form films, which is facilitated by the lower T_g nBA component that maintains an adequate free volume for temperature-responsive DL-HMPMA segments, coalesced films exhibited 3D directional responsiveness to temperature. While shrinkage occurs in the $x-y$ plane directions (length and width, respectively), expansion in the z direction (thickness) above II-LCST is observed. Computer thermodynamics molecular simulations combined with the experimental data showed that conformational changes of the side chains and the collapse of the p(DL-HMPMA/nBA) copolymer backbone are responsible for directional temperature responsiveness. To the best of our knowledge, this is the first study that shows selective 3D directional temperature-responsiveness of polymer films. These studies also show that the total free energy (G) of the system increases by 150 kcal/mol which results from the diminishing entropic term above II-LCST which, in addition to polar and hydrogen bonding interactions, contributes to conformational changes near II-LCST.

Introduction

While the majority of studies dealing with stimuli-responsive polymers focused on polymeric solutions, it is significantly more challenging to develop stimuli-responsive polymeric films.[1,2] In order for macromolecular segments to respond to external or internal stimuli, it is necessary to provide adequate spatial conditions which are easily attainable in solutions, where Brownian motion of solvent molecules requires relatively low energy for macromolecular segments to be displaced by solvent molecules. In contrast, in a solid phase, the challenge is to design a polymer network that upon stimuli will be capable of rearranging macromolecular segments while maintaining solid-state properties. Examples are hydrogels[3,4] which exhibit stimuli-responsive properties resulting from low-glass transition temperature (T_g) components providing an excess of free volume that facilitates the transport of individual components. In view of these considerations, it is of scientific and technological interest to design and develop polymers that would exhibit stimuli-responsiveness, while maintaining mechanically stable polymer networks. Although a chemical makeup of macromolecular segments formulates a prerequisite for stimuli-responsiveness of a given polymer, localized low T_g environments in the interfacial regions[5,6] favor stimuli-responsive macromolecular rearrangements in a solid state, thus facilitating spatial requirements for suitable collision frequencies to facilitate metastable equilibria.

A well-known temperature responsive poly(*N*-isopropylacylamide) (PNIPAAm) has been examined in numerous studies,[7−9] but recently poly(*N*-(DL)-(1-hydroxymethyl) propylmethacrylamide (p(DL-HMPMA)) was prepared which also exhibits temperature responsiveness in an aqueous phase with lower critical solution temperature (LCST) at approximately 35 °C.[10−12] The primary difference between PNIPAAm and p(DL-HMPMA) is that the latter possesses chiral centers and hydroxyl functional groups, which closely mimics structural features of proteins, and the presence of hydrophilic hydroxyl groups may be useful in controlling the rate of drug delivery.[13−15] One common undesirable feature of PNIPAAm and p(DL-HMPMA) polymers is their relatively high T_g which make colloidal particles coalescence under ambient conditions challenging.

In an effort to overcome this obstacle while maintaining temperature-responsive characteristics, one approach is to prepare copolymers containing the stimuli-responsiveness of DL-HMPMA and other segments that would allow coalescence. For that reason we copolymerized DL-HMPMA and *n*-butyl acrylate (nBA) monomers (T_g of p(nBA) homopolymer is ∼ −46 °C) and examined the stimuli-responsive characteristics of colloidal particles as well as coalesced p(DL-HMPMA/nBA) films. These studies consist of two parts: part I focuses on the synthesis and stimuli-responsiveness of p(DL-HMPMA/nBA) colloidal particles in an aqueous phase, whereas part II is devoted to directional temperature responsiveness of coalesced p(DL-HMPMA/nBA) films and conformational changes resulting from temperature changes.

Experimental Section

N-(DL)-(1-hydroxymethyl) propylmethacrylamide (DL-HMPMA) was purchased from Eastern Systems, Inc. Sodium dioctylsulfosuccinate (SDOSS), *n*-butyl acrylate (nBA), and potassium persulfate (KPS) were purchased from Aldrich Chemical Co. P(DL-HMPMA/nBA) copolymer was synthesized using the semicontinuous emulsion polymerization process outlined elsewhere[16] which was adapted for a small scale polymerization. The reaction flask was immersed in a water bath preheated to 72 °C and purged continuously with N_2 gas. The reactor was first charged with 23 mL of double dionized

* Author to whom all correspondence should be addressed.

10.1021/ma702101m CCC: $40.75
Published on Web 12/18/2007

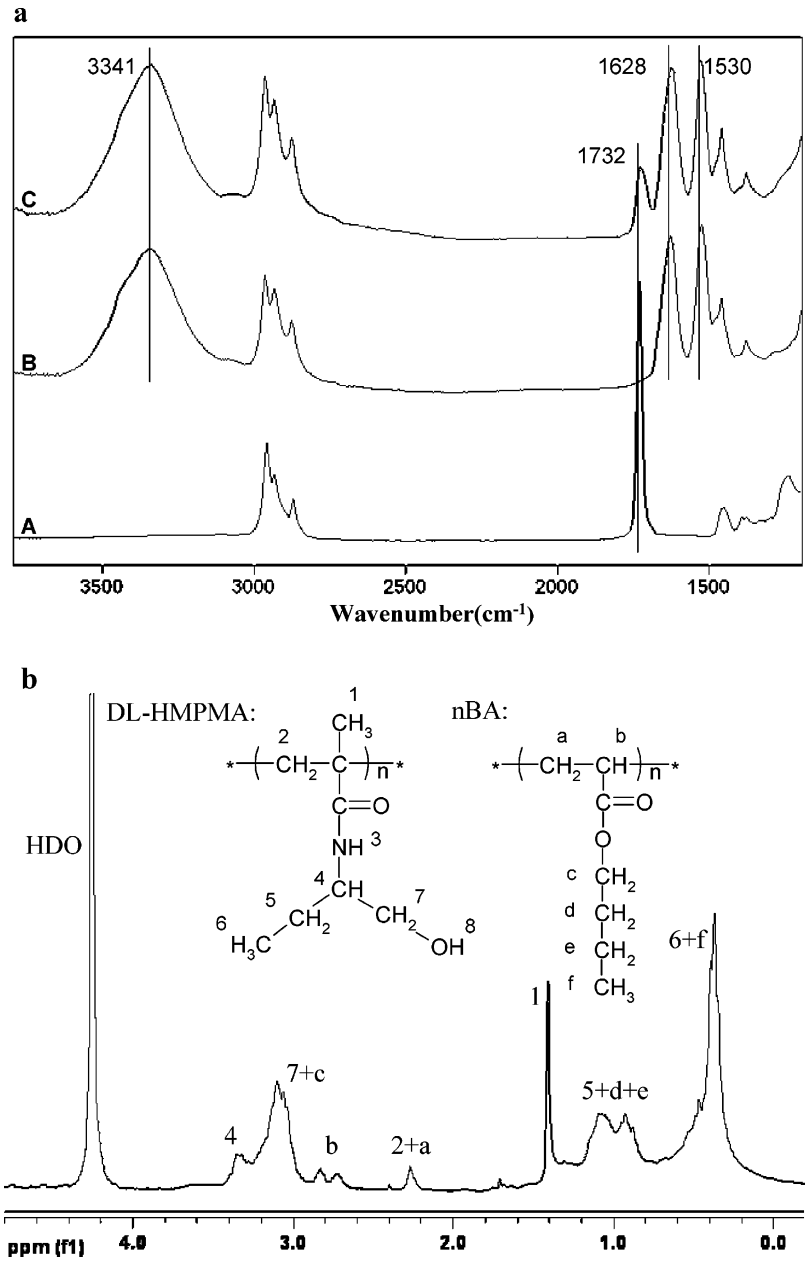

Figure 1. (a) ATR FT-IR spectra of A, pnBA; B, p(DL-HMPMA); C , p(DL-HMPMA/nBA) and (b) ^{1}H NMR spectrum of p(DL-HMPMA/nBA) in D_2O.

(DDI) water, and after purging N_2 for 30 min, the content was stirred at 350 rpm. At this point, pre-emulsion (DDI, SDOSS, and monomers) and the initiator solution (DDI and KPS) were fed at 0.119 and 0.050 mL/min into the vessel over a period of 3.5 h and 4 h, respectively. After completion of the initiator feeding, the bath temperature was increased to 85 °C and the reaction was continued for an additional hour. The resulting colloidal dispersion was filtered after cooling to ambient temperature. P(DL-HMPMA) and p(nBA) homopolymers were prepared using the same method.

Particle size analysis was performed using a Microtrac Nanotrac particle size analyzer (model NPA 250) with an accuracy of ±10 nm. To determine turbidity as a function of temperature, colloidal dispersions were diluted with DDI water to 2% w/w solution and monitored at 500 nm wavelength using a Varian Cary 500 Scan UV−vis NIR spectrophotometer. DDI water was utilized as the reference background, and each solution was allowed to equilibrate for 30 min at a given temperature before measurements.

Molecular weight was determined using gel permeation chromatography (Waters, Inc.) equipped with a 515 HPLC pump and a 2414 model refractive index detector. Each sample was precipitated in tetrahydrofuran (THF) and eluted through a 5 μm polypore column. Elution times were referenced against polystyrene standards, and molecular weights of p(DL-HMPMA/nBA) copolymer and p(DL-HMPMA) homopolymer were 173 000 and 186 000 g/mol, respectively.

Proton NMR spectra were acquired using a Varian Mercury 300 MHz NMR spectrometer. Typical measurement conditions involved 45° pulse, relaxation delay 1 s, acquisition time of 1.998 s. Each spectrum represents the co-addition of 64 scans. For each measurement, 5.8% w/v of copolymer was dissolved in deuterium oxide (D_2O) and the temperature was controlled by a Bruker Variable Temperature Unit equipped with a Eurotherm 818 Controller. Before data acquisition, each sample was equilibrated at a given temperature for 30 min.

Microscopic attenuated total reflectance Fourier transform infrared (ATR FT-IR) spectra were collected on a Bio-Rad FTS-6000 FT-IR single-beam spectrometer set at 4 cm^{-1} resolution equipped with a deuterated triglycine sulfate (DTGS) detector. A 2 mm Ge crystal with a 45° face angle maintaining constant contact pressure between the crystal and the specimens was used. An

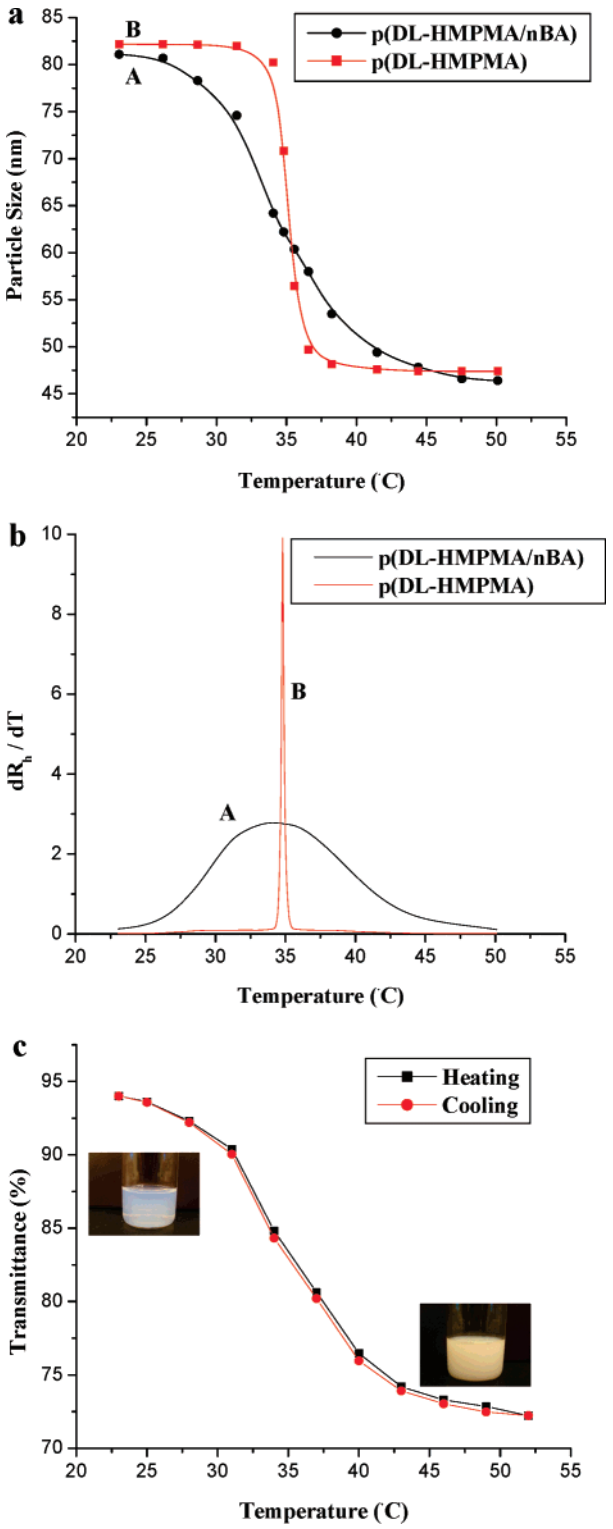

Figure 2. (a) Particle size and (b) its first derivative of A, p(DL-HMPMA/nBA); B, p(DL-HMPMA) plotted as a function of temperature; (c) % transmittance plotted as a function of temperature, (■) heating; (●) cooling.

amount of 1 μL of colloidal dispersion was placed directly on the Ge crystal and allowed to dry at least 1 h to form a layer of film on the crystal. Each spectrum was collected on the film−substrate (F−S) interface with attached heating elements and represented 100 co-added scans ratioed to 100 scans collected on an empty ATR cell. All spectra were corrected for spectral distortions by Q-ATR software using the Urban−Huang algorithm.[17] Polarization experiments were conducted to determine the preferential orientation of surface groups near the film−air (F-A) and film−substrate (F−S) interfaces. For this reason the 0° (TE) and 90° (TM) polarizer was utilized, where TE and TM are transverse electric and transverse magnetic vectors of the incidence light polarized at 0° and 90° with respect to the sample surface.[17]

Polymeric films were prepared by casting colloidal dispersions onto the poly(tetrafluoroethylene) (PTFE) substrate and allowed to coalescence at 80% relative humidity (RH) for 72 h at 22 °C in an environmental chamber. In a typical experiment, approximately 300 μm thick films were obtained and 20 × 10 mm sections were used for dimensional change experiments. Each specimen was equilibrated for 8 h at a given temperature before measuring the dimensional changes using a micrometer (Mitutoyo Co.) with a precision of ±0.1 μm. Each data point shown in Figure 7 represents an average of three measurements.

Surface morphologies of coalesced films were analyzed using an FEI Quanta 200 scanning electron microscope (SEM). All specimens were sputter coated with 5 nm thick gold under an argon atmosphere using Emitech K550X gold sputter coater and SEM analysis was performed using a 20 kV accelerated voltage.

Quantum mechanical semiempirical calculations were conducted using Material Studio software (Accerlrys Inc., version 4.1). Computer modeling simulations were performed using a classical (Newton) molecular dynamics theory combined with the COMPASS force field conditions. In the first step, we created an infinite polymer long chain containing DL-HMPMA and nBA monomer units using 3D periodic boundary conditions, such that the local thermoinduced flux was set proportional to the local atom density changes and local thermodynamic driving forces of the chemical potential. In an effort to determine thermodynamic responses of molecular segments, a 25 × 25 × 25 Å periodic unit cell was constructed and temperature was the control parameter to simulate the heat exchange with the environment.

Results and Discussion

In an effort to establish chemical composition resulting from the synthesis of DL-HMPMA and nBA monomers described in the Experimental Section, IR and ^{1}H NMR analyses were performed. Figure 1a, traces A−C illustrate ATR FT-IR spectra of p(nBA) and p(DL-HMPMA) homopolymers, as well as p(DL-HMPMA/nBA) copolymer prepared for the purpose of these studies. As seen in trace A, the band at 1732 cm^{-1} corresponding to the C═O stretching vibrations of ester groups[18−20] of p(nBA) as well as the bands at 3341, 1628, and 1530 cm^{-1} due to the O−H stretching vibrations and secondary amide C═O and N−H stretching[18−20] of p(DL-HMPMA) are observed. Further confirmation of copolymerization is illustrated in the ^{1}H NMR spectrum of p(DL-HMPMA/nBA) recorded at 25 °C in D_2O. As shown in Figure 1b, typical resonances due to DL-HMPMA and nBA units[10,19−22] are identified with the exception of the signals due to N−H and O−H protons owning to their proton exchange with water. A strong resonance at 4.3 ppm is due to the HDO signal.

Although these data demonstrate that using the feed ratio of 1:1 in the free radical semi-continuous process, copolymerization was achieved, and reactivity ratios for both monomers suggest that this process results in a random DL-HMPMA rich copolymer. Since an ultimate objective of these studies is to develop stimuli-responsive films and advance limited knowledge of film formation of stimuli-responsive colloidal dispersions, the remaining parts of this manuscript are organized into two sections: solution (I) and solid state (II) aspects of p(DL-HMPMA/nBA) copolymers. While section I is devoted to stimuli-responsive behavior of p(DL-HMPMA/nBA) colloidal particles in an aqueous phase, section II examines coalescence, multidirectional responses, and conformational changes of p(DL-HMPMA/nBA) films as a function of temperature.

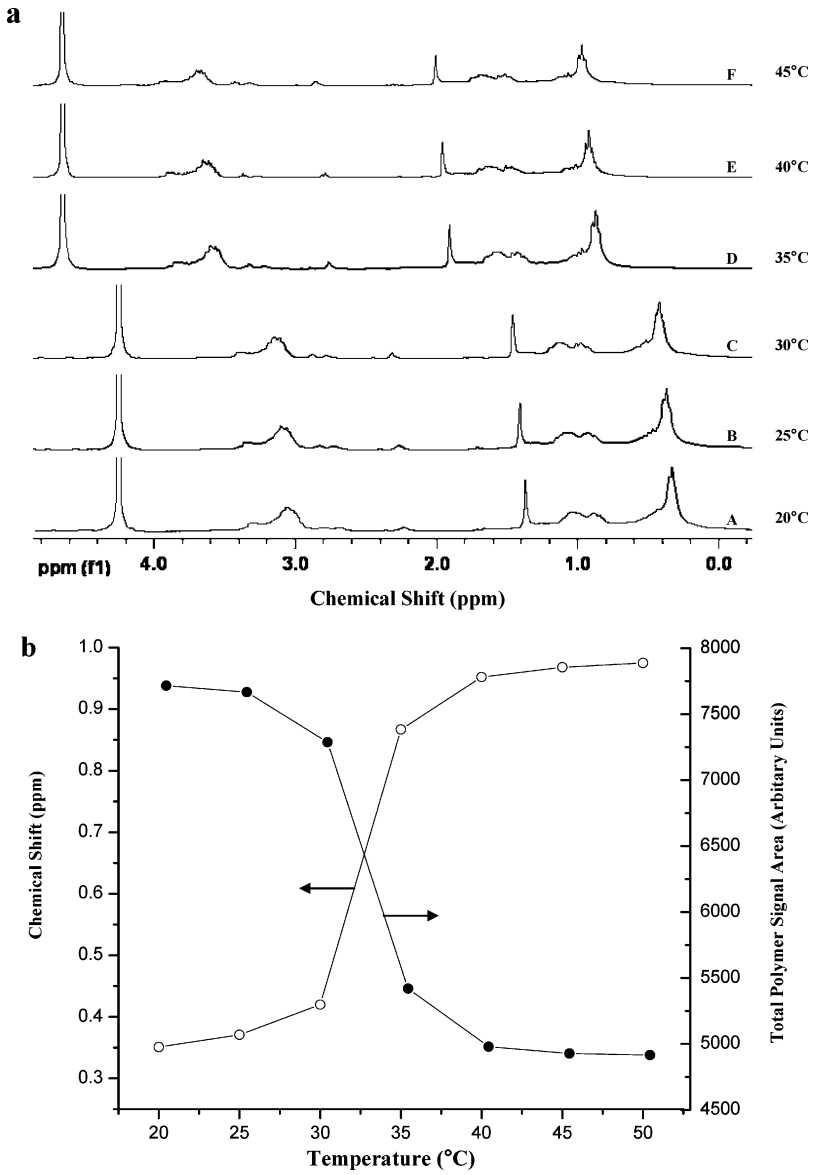

Figure 3. (a) ^{1}H NMR spectra recorded as a function of temperature; traces A, 20 °C; B, 25 °C; C, 30 °C; D, 35 °C; E, 40 °C; F, 45 °C; (b) chemical shift of methyl groups and integrated total resonance peak area plotted as a function of temperature, (○) chemical shift; (●) total resonance peak area.

I. Solution Behavior of Colloidal p(DL-HMPMA/nBA) Dispersions. In an effort to establish thermal-responsiveness of p(DL-HMPMA/nBA) copolymer colloidal particles, the particle size, UV−vis, and ^{1}H NMR analysis were conducted as a function of temperature. As shown in Figure 2a, as the temperature increases from 22 to 50 °C, the particle size of the colloidal dispersions decreases from 81 to 47 nm which, according to the literature,[23−25] results from hydrogen bonding and hydrophobic interaction changes, which are believed to be the main contributors to temperature sensitivity. However, unlike the homopolymer of p(DL-HMPMA), which exhibits a narrow transition at 35 °C shown in Figure 2a, the particle size of p(DL-HMPMA/nBA) copolymer decreases gradually over the 27−37 °C temperature range, which is attributed to the presence of nBA units. The first derivative of the particle size curves is plotted in Figure 2b and as expected, the bell shape curve for p(DL-HMPMA/nBA) is observed, whereas the p(DL-HMPMA) homopolymer exhibits a single temperature peak. These data illustrate that copolymerization of nBA and DL-HMPMA monomers broadens the LCST transition, making it like the secondary transition. For that reason we will refer to this transition as the second-order low critical solution temperature (II-LCST) transition. Turbidity measurements exhibit parallel behavior,[26] and as shown in Figure 2c, % transmittance changes are also reversible. This phenomenon is visually illustrated on the enclosed photographs, where clear and turbidity/translucent dispersions are observed upon reversible cooling and heating cycles of the colloidal solutions.

^{1}H NMR spectra of p(DL-HMPMA/nBA) colloidal dispersions are also sensitive to temperature changes.[27−30] As shown in Figure 3a, all resonances shift to lower magnetic fields as the temperature increases, with the most pronounced shifts detected between 30 and 40 °C. As expected, this behavior is attributed to local magnetic field changes around a nuclei, which results from conformational changes and subsequently electronic structure changes induced by temperature.[31] When temperature increases, copolymer chains rearrange from an extended to a collapsed state, which affects local magnetic and environmental shielding effects, causing the resonance shifts toward lower magnetic fields. Furthermore, the intensity of the ^{1}H resonance decreases as the temperature increases, which is attributed to reduced molecular mobility of the polymer segments in the

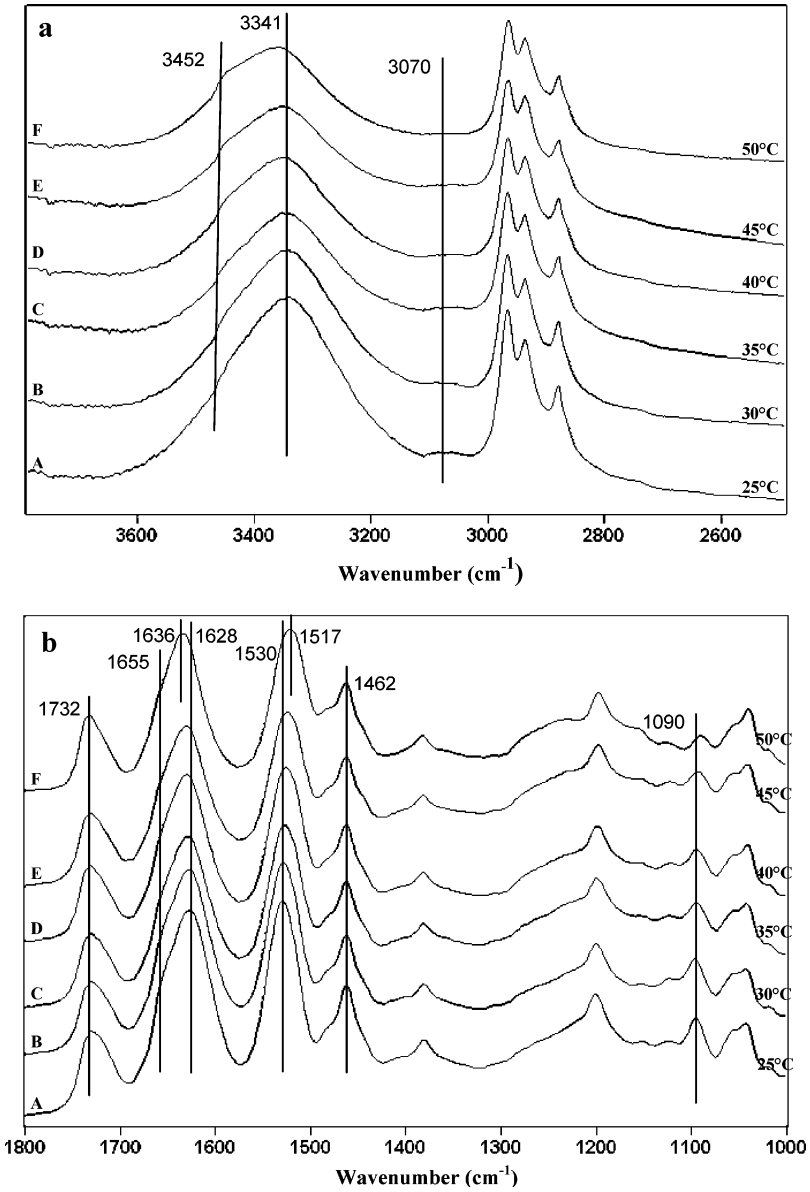

Figure 4. ATR FT-IR spectra of p(DL-HMPMA/nBA) recorded as a function of temperature in (a) 1800−1000 and (b) 3800−2500 cm^{-1} regions; traces A, 25 °C; B, 30 °C; C, 35 °C; D, 40 °C; E, 45 °C; F, 50 °C.

collapsed state. As an example, Figure 3b illustrates chemical shift changes of the methyl side groups and the integrated total polymer signal area plotted as a function of temperature. As seen, chemical shifts and the integrated band areas of the resonances also occur between 27 and 37 °C, which parallels the II-LCST transition observed in the particle size and turbidity measurements. In summary, copolymerization of DL-HMPMA monomer with nBA monomer maintains stimuli-responsive characteristics which is a prerequisite for creating stimuli-responsive films.

II. Solid-State p(DL-HMPMA/nBA) Behavior. As stated in the Introduction, the challenge is to develop stimuli-responsive polymeric films while maintaining the integrity of a polymeric network. For that reason, p(DL-HMPMA/nBA) colloidal particles were allowed to coalesce and such films were exposed to temperature changes. Figure 4a,b illustrate ATR FT-IR spectra of p(DL-HMPMA/nBA) copolymer films in two spectral regions recorded as a function of temperature. The bands at 3341 (O−H/N−H stretch), 3070 (amide II, overtone), and 2840−3020 (C−H stretch) in the 3800−2500 cm^{-1} region as well as the bands at 1628 (C═O amide I), 1530 (N−H amide II), 1462 (CH_2/−OCH_2 def), and 1090 (C−O str) in 1800−1000 cm^{-1} region decrease as the temperature increases. As anticipated, these changes are attributed to the rearrangement and collapse of polymeric chains above II-LCST.[32−34] At the same time, selected bands shift as the temperature increases, which reflects changes in molecular rearrangements and interactions. Upon temperature changes, partial intermolecular hydrogen bonds gradually break down and generate intramolecular hydrogen bonds which are manifested by relative intensity increases of the bands at 3452 and 1655 cm^{-1}.[20,35] However, no intensity decrease or significant shifts are observed for the 1732 cm^{-1} band due to C═O ester stretching vibrations of the nBA component of the p(DL-HMPMA/nAB) copolymer. These observations suggest that hydrogen bonds of the nBA segments are not involved in the chain rearrangements induced by temperature changes. However, diminished band intensities of the C−H stretching vibrations due to CH_2/CH_3 segments above II-LCST indicate that these segments participate in temperature responses.

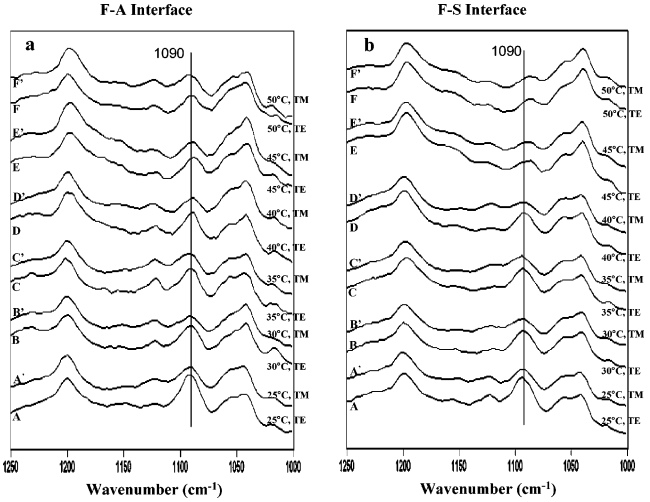

Figure 5. Polarized ATR FT-IR spectra recorded from (a) F−A interface and (b) F−S interface; traces A, 25 °C, TE; A′, 25 °C, TM; B, 30 °C, TE; B′, 30 °C, TM; C, 35 °C, TE; C′, 35 °C, TM; D, 40 °C, TE; D′, 40 °C, TM; E, 45 °C, TE; E′, 45 °C, TM; F, 50 °C, TE; F′, 50 °C, TM.

On the basis of these spectroscopic observations, one may hypothesize possible structural changes resulting from the temperature changes. Because of the free volume introduced by the lower T_g nBA component of the p(DL-HMPMA/nBA) copolymer, rotational freedom of the butyl ester pendent groups provides an adequate space for polymer chain rearrangements, but conformational changes occur within the moiety of DL-HMPMA of the copolymer. Although the hydrophobic backbone and the side groups of the DL-HMPMA component may collapse as temperature increases, butyl ester pendent groups may be moved away from the polymer backbone, thus utilizing the free volume to facilitate conformational changes. If this hypothesis is indeed valid, orientation changes of the side groups should occur as a function of temperature. To examine this behavior, orientation changes were monitored as a function of temperature using polarized ATR FT-IR spectroscopy. The results of these experiments are illustrated in Figure 5a,b which show a series of polarized ATR FT-IR spectra of p(DL-HMPMA/nBA) recorded from the F−A and F−S interfaces. As seen, higher intensity of the 1090 cm^{-1} band due to C−O stretching modes of the side groups in the TE mode indicates their preferential parallel orientation below the II-LCST. However, the same band in the TE mode of polarization decreases gradually with the increasing temperature, and the same changes are observed at the F−A and F−S interfaces. With the use of these measurements, the dichroic ratio (R) values were determined, and the R values decrease from 1.58 at 25 °C to 0.64 at 50 °C at the F−A interface and from 1.60 at 25 °C to 0.66 at 50 °C at the F−S interface,[36] thus indicating that, indeed, the orientation of the side groups changes from preferentially parallel to perpendicular as a result of temperature induced expansion and collapse.

To further understand the molecular changes and dynamics of p(DL-HMPMA/nBA) temperature response, computer modeling experiments using molecular thermodynamics simulations were employed. The p(DL-HMPMA/nBA) unit cells were constructed by packing energy minimized polymer chains in a random sequence of DL-HMPMA and nBA monomer units under 3D periodic boundary conditions, while details of the computational analysis was provided in the Experimental Section. Visualization of the results are depicted in Figure 6a. As temperature increases above II-LCST, the unit cells become denser and significant conformational changes occur. As a result of the chain collapse, the calculated total energy of the system (G), which is comprised of the potential energy (E_{pot}) and kinetic energy (E_{kin}), increases by 150 kcal/mol (from 1826 to 1976 kcal/mol) when temperature increases from 25 to 50 °C. At the same time, E_{pot} changes by 82 kcal/mol (from 686 to 768 kcal/mol) and E_{kin} by 68 kcal/mol (from 1140 to 1208 kcal/mol). Since the E_{pot} accounts for conformational changes of the unit cell and E_{kin} for the kinetic energy which is proportional to temperature, the total free energy increase results from diminishing entropic term ($\Delta G = \Delta H - T\Delta S$, assuming that ΔH remains only slightly affected by temperature). Furthermore, these molding experiments show that during this process, the volume (V) decreases by 14.2% (from 12.57 to 10.78 nm^3) and at $T >$ II-LCST butyl ester side groups still occupy a significant volume and are capable of rotating, while DL-HMPMA component collapses to form bulky spheres. The inserts a′ and a″ in Figure 6a depict conformational changes along the polymer backbone axis (dashed line) and their significant conformational changes of nBA as well as the collapse of DL-HMPMA. It is also apparent that the backbone buckles inward which is the contributing factor to the overall volume decrease. On the basis of these calculations as well as the spectroscopic analysis discussed above, the model depicting this behavior is schematically shown in Figure 6b, where the circles correspond to the free volume changes associated with the thermal response of DL-HMPMA or nBA segments of the copolymer. Below II-LCST the copolymer backbone is extended and the side chains of DL-HMPMA (A) and nBA (B) exhibit fairly high freedom. However, above II-LCST the backbone collapses and conformational changes of both side groups result in the collapsed state.

Using semiempirical calculations we also calculated vibrational energy changes of the experimentally detected IR bands that are most temperature sensitive to conformational changes. The bands of particular interest are due to the C═O of ester and amide I linkages at 1732 and 1628 cm^{-1}, respectively, as well as the 1530 cm^{-1} band due to N−H bending vibrations of the amide II. As shown in Figure 4b, experimental data show that the 1732 cm^{-1} band exhibits no sensitivity to II-LCST. However, the amide I and II bands shift and become weaker in the following order: amide I at 1628 cm^{-1} shifts to 1636 cm^{-1}, whereas amide II at 1530 cm^{-1} shifts to 1517 cm^{-1}. At the same time, the intensities of both bands decrease. Using the model depicted in Figure 6a, we calculated IR changes of these bands which showed the same trends; that is, above II-LCST, the band intensities diminish and, at the same time, the 1730 cm^{-1} band due to C═O esters remains unchanged. The amide I and II bands shift from 1636 to 1648 cm^{-1} and from 1538 to 1527 cm^{-1}, respectively. While these data obtained from theoretical calculations depicted in Figure 6a are in agreement with the experimental data, it should be noted that if polar or hydrogen-bonding interactions were solely responsible for the II-LCST transition, as proposed in the literature, the magnitude of the spectroscopic changes would be significantly greater in both experimental and computational analysis. As shown above, this is not the case and the fact that the entropic term appears to significantly contribute to energy changes, packing of hydrophobic segments containing CH_2/CH_3 segments as well as the buckling of the polymer backbone are significant contributors to the energy and volume changes.

As indicated earlier, spectroscopic analysis indicated orientation changes of p(DL-HMPMA/nBA) copolymer components. The question is wheather these changes affect macroscopic film dimensions changes and how they appear to be important. In

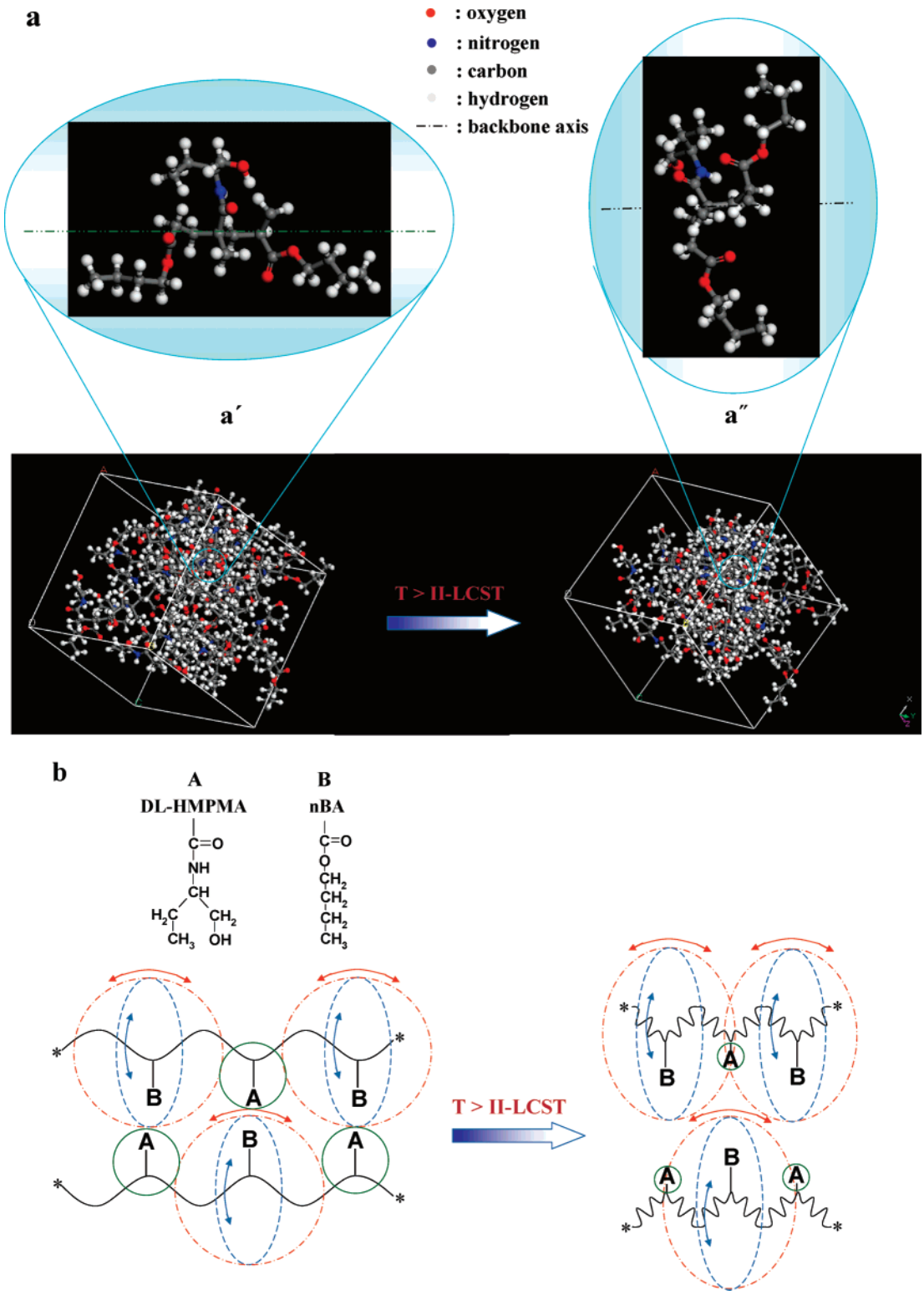

Figure 6. Results of computer simulations: (a) volume and conformational changes resulting from temperature changes; inserts a′ and a″ illustrate unit cells below and above II-LCST; (b) schematic representation of volume changes resulting from temperature; arrows indicate rotations of the nBA side groups and circles represent free volume changes.

an effort to determine directional volume transitions in solid p(DL-HMPMA/nBA) films as a function of temperature, dimensional changes of coalesced films were measured in the *x*, *y*, and *z* directions. Figure 7, curves a, b, and c illustrate relative changes in the *x*, *y*, and *z* directions, respectively, plotted as a function of temperature. Interestingly enough, the length and width (*x* and *y* directions) diminish but thickness of the film (*z* direction) increases. These changes occur again in the 27−37 °C temperature range which correspond to the II-LCST and agree with the data discussed in Figures 2 and 3. It should be also noted that dimensional changes in the *z* direction are significantly smaller, thus the overall total volume of the film decreases as a function of temperature, which is illustrated in Figure 7d. When going from 22 to 50 °C, the total observed volume decrease is 18.5%, which agrees with the computer modeling data (14.2%). It should be also noted that these

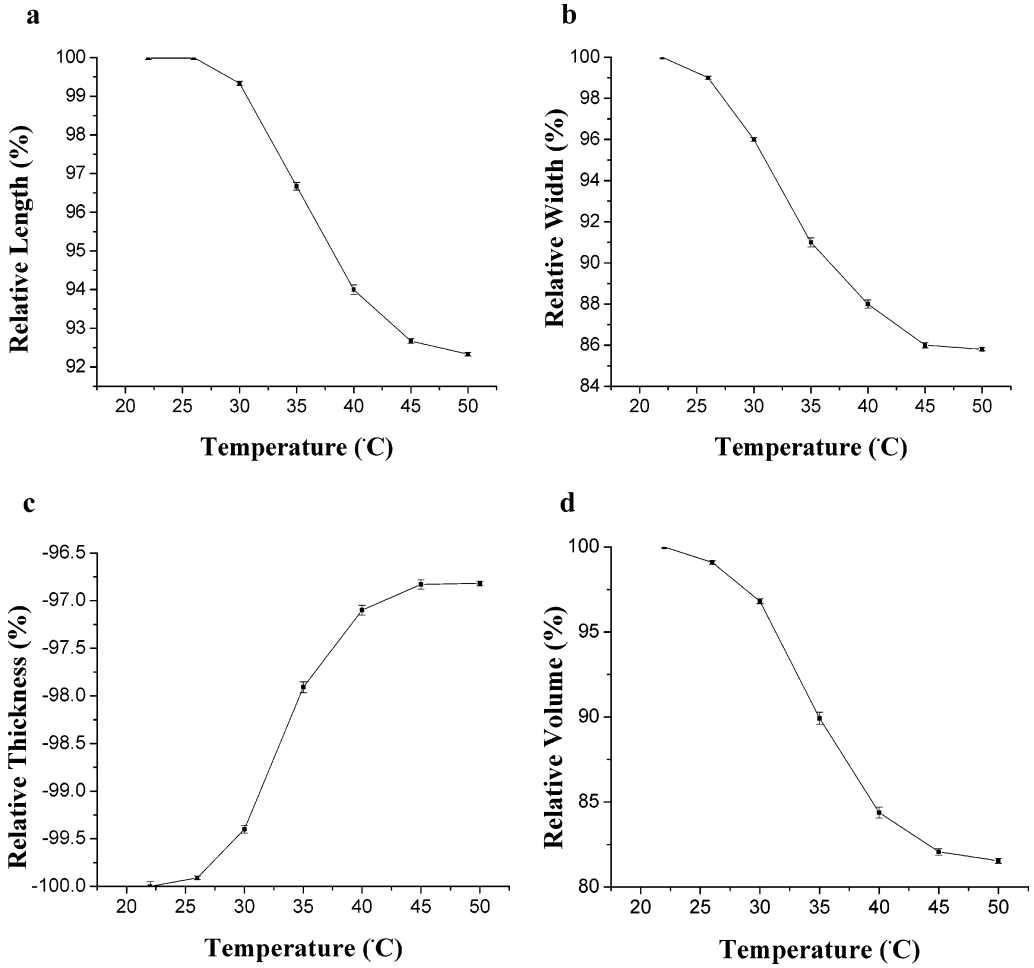

Figure 7. 3D directional thermal response of p(DL-HMPMA/nBA) films: (a) film length, (b) film width, (c) film thickness, and (d) total film volume changes plotted as a function of temperature.

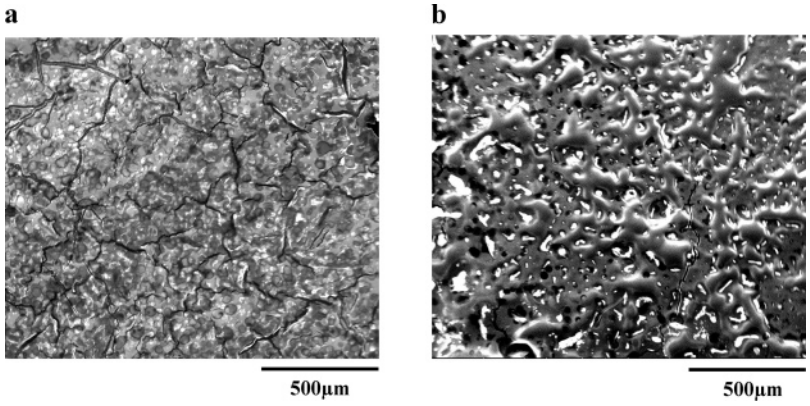

Figure 8. SEM images of p(DL-HMPMA/nBA) films coalesced at (a) 22 °C and (b) 40 °C.

changes affect surface morphologies. As shown in Figure 8a, the SEM image of the p(DL-HMPMA/nBA) film surface coalesced at 22 °C exhibits uniform surface morphology, but upon coalescence at 40 °C, surface buckling is observed due to shrinkage in the $x-y$ and expansion in the z directions. This is shown in Figure 8b.

On the bais of these data, the model depicted in Figure 9 is proposed which accounts for the 3D directional thermal-responsive behavior of p(DL-HMPMA/nBA) copolymer films. As shown, expansions and collapses of polymeric segments in p(DL-HMPMA/nBA) occur as a function of temperature. Below II-LCST, copolymer chains are extended and adopt a lateral configuration, which is facilitated by the lower T_g of the nBA component and the presence of hydrophilic groups. Under these conditions copolymer chains are able to spread out in the $x-y$ directions, while reducing their size in the thickness z direction. As the temperature increases above II-LCST, DL-HMPMA components collapse, which are facilitated by the buckling of the copolymer hydrophobic backbone, thus allowing the side groups to expand in the z direction. For this reason, the film thickness increases and shrinkage occurs in the $x-y$ directions, thus causing surface buckling. Water molecules play an important role in 3D directional temperature-responsiveness and their participation provides an environment with metastable equilibrium conditions for polymer chain rearrangements.

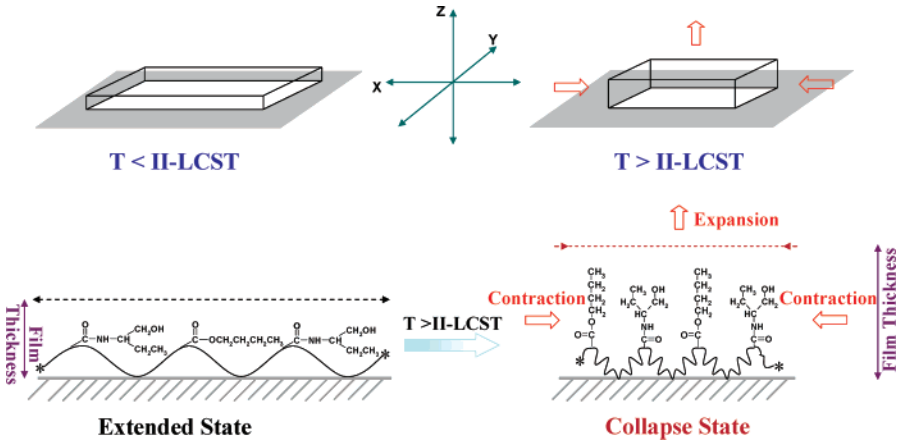

Figure 9. Schematic diagram depicting 3D directional thermal response of p(DL-HMPMA/nBA) films.

Conclusions

In these studies we synthesized novel p(DL-HMPMA/nBA) colloidal particles that retain temperature-responsive characteristics with the II-LCST in the 27−37 °C temperature range. The particle size of p(DL-HMPMA/nBA) aqueous dispersions diminishes from 81 to 47 nm as the temperature increases. When p(DL-HMPMA/nBA) colloidal particles coalesced to form films, temperature-responsiveness is maintained by the lower T_g nBA component which provides sufficient free volume for spatial rearrangements. Computer modeling experiments also showed that total free energy (G) increases by 150 kcal/mol, and in addition to relatively weak hydrogen bonding and polar interactions, entropic components play an important role in the conformational changes near II-LCST. P(DL-HMPMA/nBA) films also exhibit 3D directional responses to temperature, with shrinkage in the $x-y$ plane and expansion in the thickness (z) directions. Participation of water molecules in p(DL-HMPMA/nBA) films provides environmental conditions with metastable equilibrium to allow II-LCST rearrangements.

Acknowledgment. This work was primarily supported by the MRSEC Program of the National Science Foundation under Award No. DMR 0213883. The authors are also thankful to the National Science Foundation Major Research Instrumentation Program under the Award No. DMR 0315637 for partial financial support of these studies.

References and Notes

(1) Urban, M. W. *Polym. Rev.* **2006**, *46*, 329−339.
(2) Urban, M. W.; Lestage, D. *Polym. Rev.* **2006**, *46*, 445−466.
(3) Qiu, Y.; Park, K. *Adv. Drug Delivery Rev.* **2001**, *53*, 321−339.
(4) Osada, Y.; Gong, J. P.; Tanaka, Y. *J. Macromol. Sci., Polym. Rev.* **2004**, *44*, 87−112.
(5) Angell, C. A.; Ngai, K. L.; McKenna, G. B.; McMiuan, P. F.; Martin, S. W. *J. Appl. Phys.* **2000**, *88*, 3113−3157.
(6) Priestley, R. D.; Ellison, C. J.; Broadbelt, L. J.; Torkelson, J. M. *Science* **2005**, *309*, 456−459.
(7) Pelton, R. H. *Colloids Surf., B* **1986**, *20*, 247−256.
(8) Pelton, R. H. *Adv. Colloid Interface Sci.* **2000**, *85*, 1−33.
(9) Alarcon, C.; Pennadam, S.; Alexander, C. *Chem. Soc. Rev.* **2005**, *34*, 276−285.
(10) Aoki, T.; Murematsu, M.; Torii, T.; Sanui, K.; Ogata, N. *Macromolecules* **2001**, *34*, 3118−3119.
(11) Aoki, T.; Murematsu, M.; Nishina, A.; Sanui, K.; Ogata, N. *Macromol. Biosci.* **2004**, *4*, 943−949.
(12) Seto, Y.; Aoki, T.; Kunugi, S. *Colloid Polym. Sci.* **2005**, *283*, 1137−1142.
(13) Gutowska, A.; Bae, Y. H.; Feijen, J.; Kim, S. W. *J. Controlled Release* **1992**, *22*, 95−104.
(14) Kaneko, Y.; Nakamura, S.; Sakai, K.; Aoyagi, T.; Kikuchi, A.; Sakurai, Y.; Okano, T. *Macromolecules* **1998**, *31*, 6099−6105.
(15) Ebara, M.; Aoyagi, T.; Sakai, K.; Okano, T. *J. Polym. Sci., Part A: Polym. Chem.* **2001**, *39*, 335−342.
(16) Lestage, D.; Urban, M. W. *Langmuir* **2005**, *21*, 2150−2157.
(17) Urban, M. W. *Attenuated Total Reflectance Spectroscopy of Polymers*; Theory and Practice: Washington, DC, 1989.
(18) Socrates, G. *Infrared and Raman Characteristic Group Frequencies: Tables and Charts*, 3rd ed.; John Wiley and Sons Ltd: New York, 2001.
(19) Pretsch, E. B. P.; Affolter, C. *Structure Determination of Organic Compounds: Tables of Spectral Data*, 3rd ed.; Springer: New York, 2000.
(20) Lin-Vien, D.; Colthup, N. B.; Fateley, W. G.; Grasselli, J. G. *The Handbook of Infrared and Raman Characteristic Frequencies of Organic Molecules*; Academic Press: San Diego, CA, 1991.
(21) Landfester, K.; Spiegel, S.; Born, R.; Spiess, H. W. *Colloid. Polym. Sci.* **1998**, *276*, 356−361.
(22) Brar, A. S.; Pradhan, D. R.; Hooda, S. *J. Mol. Struct.* **2004**, *699*, 39−45.
(23) Gil, E. S.; Hudson, S. M. *Prog. Polym. Sci.* **2004**, *29*, 1173−1222.
(24) Aoyagi, T.; Ebara, M.; Sakai, K.; Okano, T. *Macromolecules* **2000**, *33*, 8312−8316.
(25) Luzinov, I.; Minko, S.; Tsukruk, V. V. *Prog. Polym. Sci.* **2004**, *29*, 635−698.
(26) Kuckling, D.; Adler, H.; Arndt, K.; Ling, L.; Habicher, W. *Macromol. Chem. Phys.* **2000**, *201*, 273−280.
(27) Spevacek, J.; Hanykova, L. *Macromolecules* **2005**, *38*, 9187−9191.
(28) Rice, C. V. *Biomacromolecules: Notes* **2006**, *7*, 2923−2925.
(29) Tokuhiro, T.; Amiya, T.; Mamada, A.; Tanaka, T. *Macromolecules* **1991**, *24*, 2936−2943.
(30) Spevacek, J.; Hanykova, L.; Ilavsky, M. *Macromol. Chem. Phys.* **2001**, *202*, 1122−1129.
(31) Koenig, J. L. *Spectroscopy of Polymers*, 2nd ed.; Elsevier Science Inc: New York, 1999.
(32) Lin, S.; Chen, K.; Run-Chu, L. *Polymer* **1999**, *40*, 2619−2624.
(33) Maeda, Y.; Nakamura, T.; Ikeda, I. *Macromolecules* **2001**, *34*, 1391−1399.
(34) Maeda, Y.; Huiguchi, T.; Ikeda, I. *Langmuir* **2001**, *17*, 7535−7539.
(35) Percot, A.; Zhu, X. X.; Lafleur, M. *J. Polym. Sci., Part B: Polym. Phys.* **2000**, *38*, 907−915.
(36) Hobbs, J. P.; Sung, C. S. P.; Krishnan, K.; Hill, S. *Macromolecules* **1983**, *16*, 193−199.

MA702101M